



# T Cell Impairment Is Predictive for a Severe Clinical Course in NEMO Deficiency

Stephanie Heller<sup>1,2</sup> · Uwe Kölsch<sup>3</sup> · Thomas Magg<sup>4</sup> · Renate Krüger<sup>1</sup> · Andrea Scheuern<sup>5</sup> · Holm Schneider<sup>6</sup> · Anna Eichinger<sup>4</sup> · Volker Wahn<sup>1</sup> · Nadine Unterwalder<sup>3</sup> · Myriam Lorenz<sup>7</sup> · Klaus Schwarz<sup>7,8</sup> · Christian Meisel<sup>2,3</sup> · Ansgar Schulz<sup>5</sup> · Fabian Hauck<sup>4</sup> · Horst von Bernuth<sup>1,2,3</sup>

Received: 13 April 2019 / Accepted: 25 November 2019 / Published online: 21 January 2020  
© Springer Science+Business Media, LLC, part of Springer Nature 2020

## Abstract

**Purpose** NEMO-deficient patients present with variable degrees of immunodeficiency. Accordingly, treatment ranges from antibiotic prophylaxis and/or IgG-substitution to allogenic hematopoietic stem cell transplantation (HSCT). The correct estimation of the immunodeficiency is essential to avoid over- as well as under-treatment. We compare the immunological phenotype of a NEMO-deficient patient with a newly-described splice site mutation that causes truncation of the NEMO zinc-finger (ZF) domain and a severe clinical course with the immunological phenotype of three NEMO-deficient patients with missense mutations and milder clinical courses and all previously published patients.

**Methods** Lymphocyte subsets, proliferation, and intracellular NEMO-expression were assessed by FACS. NF- $\kappa$ B signal transduction was determined by measuring I $\kappa$ B $\alpha$ -degradation and the production of cytokines upon stimulation with TNF- $\alpha$ , IL-1 $\beta$ , and TLR-agonists in immortalized fibroblasts and whole blood, respectively.

**Results** The patient with truncated ZF-domain of NEMO showed low levels of IgM and IgG, reduced class-switched memory B cells, almost complete skewing towards naïve CD45RA<sup>+</sup> T cells, impaired T cell proliferation as well as cytokine production upon stimulation with TNF- $\alpha$ , IL-1 $\beta$ , and TLR-agonists. He suffered from severe infections (sepsis, pneumonia, osteomyelitis) during infancy. In contrast, three patients with missense mutations in *IKBKG* presented neither skewing of T cells towards naïveté nor impaired T cell proliferation. They are stable on prophylactic IgG-substitution or even off any prophylactic treatment.

**Conclusion** The loss of the ZF-domain and the impaired T cell proliferation accompanied by almost complete persistence of naïve T cells despite severe infections are suggestive for a profound immunodeficiency. Allogenic HSCT should be considered early for these patients before chronic sequelae occur.

**Keywords** Primary immunodeficiency · NEMO deficiency · immunological phenotype · T cell deficiency · CD45RA<sup>+</sup> naïve T cells

---

Fabian Hauck and Horst von Bernuth contributed equally to this work.

**Electronic supplementary material** The online version of this article (<https://doi.org/10.1007/s10875-019-00728-y>) contains supplementary material, which is available to authorized users.

---

✉ Horst von Bernuth  
horst.von-bernuth@charite.de

<sup>1</sup> Department of Pediatric Pulmonology, Immunology, and Intensive Care Medicine, Charité-Universitätsmedizin Berlin, Berlin, Germany

<sup>2</sup> Berlin-Brandenburg Center for Regenerative Therapies, Berlin, Germany

<sup>3</sup> Department of Immunology, Labor Berlin GmbH, Berlin, Germany

<sup>4</sup> Department of Pediatrics, Dr. von Hauner Children's Hospital, University Hospital LMU, Munich, Germany

<sup>5</sup> Department of Pediatrics and Adolescent Medicine, University Medical Center Ulm, Ulm, Germany

<sup>6</sup> Center for Ectodermal Dysplasias and Department of Pediatrics, University Hospital Erlangen, Erlangen, Germany

<sup>7</sup> Institute for Transfusion Medicine, University of Ulm, Ulm, Germany

<sup>8</sup> Institute for Clinical Transfusion Medicine and Immunogenetics Ulm, German Red Cross Blood Service, Ulm, Germany

## Introduction

Currently, more than 340 genetically defined, primary immunodeficiencies (PIDs) are known, including several entities which affect the activation of the nuclear factor  $\kappa$  light chain enhancer of activated B cells (NF- $\kappa$ B) pathway [1, 2]. The NF- $\kappa$ B transcription factor is composed of homo- or heterodimer protein complexes consisting of NF- $\kappa$ B1/p50 (precursor p105), NF- $\kappa$ B2/p52 (precursor p100), RelA/p65, RelB, or c-Rel and translocates into the nucleus upon activation of the canonical or the non-canonical NF- $\kappa$ B pathway [3–5]. Mainly controlled by the classical canonical pathway, NF- $\kappa$ B (p50/p65) is retained in the cytoplasm of inactive cells through the inhibitory protein I $\kappa$ B $\alpha$ . Activation of the upstream I $\kappa$ B kinase (IKK) complex IKK $\alpha$ /IKK $\beta$ /IKK $\gamma$  leads to the proteolytic degradation of I $\kappa$ B $\alpha$  and enables NF- $\kappa$ B to translocate into the nucleus and to activate the transcription of cytokine associated genes (Fig. 1). To date, genetically defined PIDs within the canonical (*MYD88*, *IRAK4*, *IRAK1*, *TIRAP*, *CARD11*, *BCL10*, *MALT1*, *RBCK1*, *RNF31*, *TNFAIP3*, *FAM105B*, *IKBKA*, *IKKBK*, *IKBK*, *NFKBIA*) [6–25] and the non-canonical pathway (*MAP3K14*, *IKBKA*) [12, 26] as well as in single components of NF- $\kappa$ B have been described (*NFKB1*, *NFKB2*, *RELA*, *RELB*) [27–30] (Fig. 1). The majority of these defects impairs the innate as well as the adaptive immune system causing increased susceptibility to infections (bacterial, mycobacterial, viral) as well as immune dysregulation.

Patients with disturbances of the regulatory subunit of the IKK complex, IKK $\gamma$  (also known as NF- $\kappa$ B essential modulator, NEMO), often but not always present with additional non-immunological phenotypes like anhidrotic ectodermal dysplasia (EDA), osteopetrosis, or lymphedema [1, 2, 6–8]. More than 100 mutations in the NEMO-encoding, X-chromosomal gene *IKBK*, have been described [31–34]. Depending on the altered functional domain, hypomorphic mutations can vary substantially in the quantity and quality of residual function [31, 32, 35]. Heterozygous amorphic mutations cause incontinentia pigmenti (IP) in female carriers (rarely also accompanied by immunodeficiency) and are lethal in hemizygous males [36–38]. The immunological core-phenotype of NEMO-deficient patients comprises reduced levels of IgG (especially IgG<sub>2</sub>), aberrant levels of IgM and IgA, deficient polysaccharide-responsiveness, low class-switched memory B cells, and impaired IL-10 production upon activation with tumor necrosis factor  $\alpha$  (TNF- $\alpha$ ). In most cases, neither amounts nor composition of subsets nor functionality of T cells are impaired and are hence rarely assessed in sufficient detail in these patients. This immunological heterogeneity results in variable clinical courses of NEMO deficiency comprising patients who require no supportive therapy, patients who are stable on antibiotic prophylaxis and/or IgG-substitution, and patients for whom HSCT seems a reasonable,

if not necessary approach [39]. However, HSCT only cures NEMO deficiency in mesoderm-derived tissues but does not correct dysregulation in ectodermal or endodermal compartments [39, 40]. In the single published cohort, the overall survival of NEMO-deficient patients after HSCT was 74% and seems worse in patients with pre-existing mycobacterial infections or colitis [39]. Therefore, the early and detailed evaluation of the immunological phenotype, comprising the innate as well as the adaptive immune system, is necessary to predict the individual prognosis.

We here report a child with a previously non-described splice site mutation in *IKBK* (IVS9 + 1G > A) causing a loss of the ZF-domain in whom we diagnosed a characteristic T cell phenotype after birth and who subsequently suffered from life-threatening severe bacterial and fungal infections. The comparison with the immunological phenotype and the less severe clinical course of three additional NEMO-deficient patients with separate amino acid exchanges in the coiled-coil 1 (CC1) domain (L80P, D113N) or in the leucine zipper (LZ) domain of NEMO (R319Q) due to missense mutations and the thorough comparison of all previously published patients with NEMO deficiency allowed us to define a T cell phenotype predictive for a severe clinical course.

## Methods

All procedures performed in studies involving human participants were in accordance with the ethical standards of the institutional and/or national research committee (Charité-Universitätsmedizin Berlin, Germany, EA2/053/08 and EA2/132/11) and with the 1964 Helsinki declaration and its later amendments or comparable ethical standards. Informed consent was obtained from all individual participants included in the study.

## Case Reports

The first patient (P1) was born to non-consanguineous Caucasian parents. His mother and elder sister had IP caused by a mutation in the intervening sequence of exon 9 (IVS9 + 1G > A). During pregnancy, an amniocentesis had been performed and revealed the same *IKBK* mutation in P1 (Fig. 2). Immediately, after birth, P1 received an antibiotic prophylaxis against bacterial infections. In his first month of life, P1 developed an EDA-like phenotype that was confirmed by a skin biopsy. At the age of 3 months, he presented a redness of his right ankle joint. Despite antibiotic treatment, he presented fever (39.4 °C), an increased level of CRP (136.7 mg/L), reduced oxygen saturation and was admitted to hospital. Levels of IgG (1.35 g/L) and IgM (0.03 g/L) were diminished (Table 1). Sepsis caused by *Enterobacter aerogenes* and a

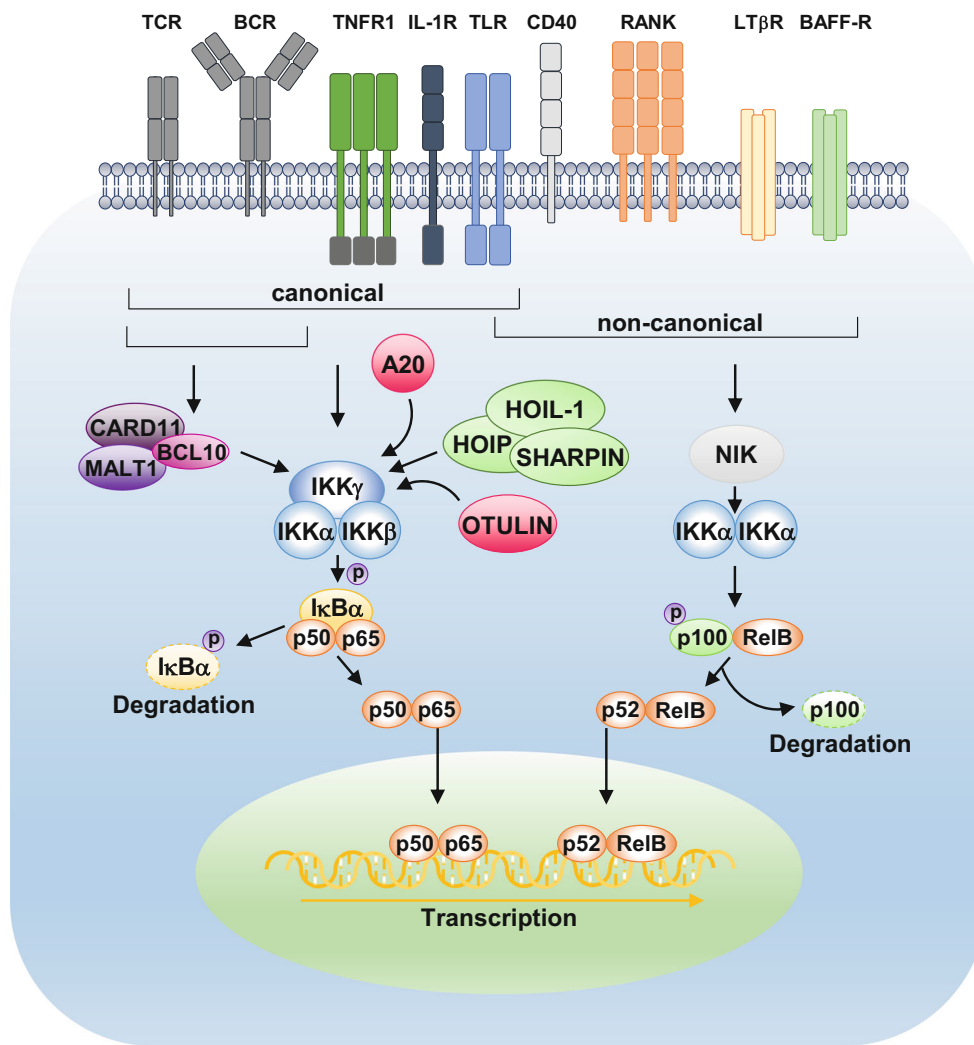


**Fig. 1** Canonical and non-canonical pathway of NF-κB. NF-κB-controlled signal transduction uses two distinct pathways, the “canonical” and the “non-canonical” one. These pathways are controlled by distinct receptors on the cell surface. The canonical pathway comprises a trimeric IκB kinase complex which consists of IKKα, IKKβ, and IKKγ (NEMO). The complex is activated by upstream mediators, like the CARD11-BCL10-MALT1 (CBM)-complex and leads to the phosphorylation and proteolytic degradation of the inhibitor IκBα whereupon NF-κB (p50/p65) migrates into the nucleus. The LUBAC-complex (consists of HOIL-1, HOIP, and SHARPIN) leads to a linear ubiquitinylation of IKKγ, whereas A20 and OTULIN act as negative regulators of the NF-κB-pathway by cleaving the ubiquitinylated chains. The non-canonical pathway implies the NF-κB-inducing kinase NIK which leads to the phosphorylation of the dimeric IKKα-complex and consequently to the transformation of the inactive precursor protein p100 to the active RelB-protein p52. The resulting NF-κB factor p52/RelB translocates into the nucleus

and activates transcription. The NF-κB pathway can be disturbed through disease-causing mutations within multiple genes. Described correlations between phenotype and genotype are listed in the OMIM database (OMIM numbers: A20/TNFAIP3\*191163, BCL10\*603517, CARD11\*607210, HOIL-1610924, HOIP 612487, IκBα\*164008, IKKα\*600664, IKKβ\*603258, IKKγ\* 300248, MALT1\*604860, NIK\*604655, OTULIN\*615712, p50\*164011, p52\*164012, p65\*164014, RelB\*604758). BCL, B cell leukemia/lymphoma; BCR, B cell receptor; CARD, caspase recruitment domain-containing protein; CD, cluster of differentiation; IκBα, NF-κB inhibitor α; IKK, IκB kinase; IL-1R, interleukin-1 receptor; LTβR, lymphotoxin β receptor; MALT, mucosa-associated lymphoid tissue lymphoma translocation protein; NIK, NF-κB-inducing kinase; TCR, T cell receptor; TLR, toll-like receptor; TNFR1, tumor necrosis factor receptor 1; RANK, receptor activator of NF-κB

*Pneumocystis jirovecii* pneumonia (PJP) were identified and treated successfully. At the age of 6 months, P1 presented a swollen right knee. Magnetic resonance imaging and a biopsy revealed an osteomyelitis caused by *Enterobacter aerogenes*. He was treated with clindamycin, cefuroxim, and meropenem. In addition, he exhibited lymphedema of his left lower leg. In consideration of his

severe clinical course, HSCT was performed at the age of 9 months (Table S1). After myeloablative conditioning (busulfan, fludarabin, thiotepe, alemtuzumab), he was transplanted with bone marrow of an unrelated HLA-compatible donor (MUD, 10/10 with non-permissive DPB1-mismatch). Prophylaxis against graft versus host disease (GVHD) consisted of mycophenolate mofetil and

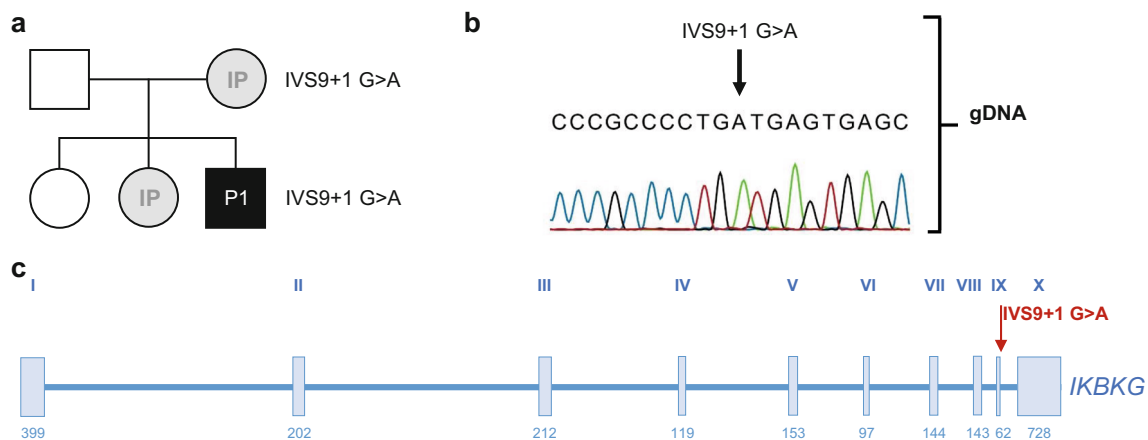


**Fig. 2** Genotype of P1. **a** Pedigree of P1. Incontinentia pigmenti-positive family members and female carriers of the *IKBKG* mutation within the intervening sequence of exon 9 (IVS9 + 1G > A) are shown in gray. The male patient P1 is shown in black. O, female; □, male. **b** Sequence analysis of *IKBKG*. The analysis (long-range PCR) was performed with

genomic DNA (gDNA) which was isolated from patient's SV40 fibroblasts. The hemizygous mutation IVS9 + 1G > A is indicated by a black arrow. **c** Schematic presentation of *IKBKG*. The NEMO-encoding gene contains 10 exons which are depicted as I–X. The mutation locus is indicated by a red arrow

cyclosporine A. Neutrophil engraftment > 500/ $\mu$ l was achieved on day +25 and thrombocyte engraftment of > 50.000/ $\mu$ l on day +35. On day +20, he developed a hepatic veno-occlusive disease/sinusoidal obstruction syndrome that quickly resolved on defibrotide. On day +152, P1 developed a severe autoimmune thrombocytopenia that was refractory to IgG-substitutions, steroids, and rituximab, however, could be treated with daratumumab. On day +246, P1 presented bloody stools and decreased amounts of hemoglobin. GVHD of the gut was confirmed by coloscopy and was treated with steroids and anti-TNF- $\alpha$ -antibodies. Furthermore, he suffered from a bacteremia (*Enterobacter aerogenes*) whereupon he received meropenem, gentamycin, and linezolid. P1 is now 2<sup>8</sup>/<sub>12</sub> years old, presents a slight retardation of his length and weight and due to chronic GVHD-colitis requires immunosuppression (JAK-inhibitors, anti-TNF- $\alpha$ -antagonists).

The second patient (P2) was born to non-consanguineous Caucasian parents. His grandmother and mother are carriers of a heterozygous *IKBKG* mutation at position 337 (c. G337A) which leads to an amino acid exchange of aspartic acid to asparagine at position 113 (p. D113N) (Fig. S1a). This mutation had been previously described in patients with IP [44] as well as in NEMO-deficient patients with PJP and CMV infections who were treated with IgG-substitutions or HSCTs, respectively [39, 45, 46]. P2 presents normal amounts of NEMO and has no signs of EDA (Fig. S1b). From his third month of life, P2 suffered from recurrent febrile lower respiratory tract infections (pneumonia, bronchitis), middle ear infections, and conjunctivitis. P2 developed relapsing and painful oral lesions caused by HSV-1 that were treated with aciclovir and valaciclovir. His peripheral blood analysis showed no

abnormalities. Immunoglobulin levels (mild hypogammaglobulinemia) as well as his antibody titer against tetanus-toxoid were inconspicuous. However, P2 developed only low amounts of polysaccharide-specific antibodies despite vaccination (Table S2). Due to the lack of specific antibodies and recurrent respiratory tract infections, P2 has been receiving regular IgG-substitutions since his 5th year of life. On regular IgG-substitution, no severe respiratory infections were observed but oral HSV-1 lesions still occur monthly. P2 is now 10<sup>1</sup>/<sub>12</sub> years old. His cousin (P2C) carries the same *IKBKG* mutation, however, exhibits normal amounts of polysaccharide-specific antibodies, suffered from no bacterial or viral infections, and is now 40<sup>5</sup>/<sub>12</sub> years old (Table S3).

Patients 3 (P3) and 4 (P4) had been described in detail previously [47, 48]. Briefly, P3 was born to non-consanguineous Caucasian parents and suffered from recurrent bacterial and viral infections (herpes labialis caused by HSV-1). He presents reduced levels of IgM and polysaccharide-specific antibodies despite several pneumococcal infections. P3 carries an amino acid exchange within the N-terminal CC1 domain of NEMO (L80P) and exhibits a reduced NEMO expression (Fig. S2a). He has been receiving IgG-substitution since his 3<sup>1</sup>/<sub>2</sub> year of life, has not developed severe infections ever since, is now 25<sup>11</sup>/<sub>12</sub> years old, is in good health, and leads an independent life (Table S4). P4 was born to non-consanguineous Caucasian parents and developed at the age of 1<sup>1</sup>/<sub>2</sub> years a cervical lymph node abscess caused by *Haemophilus influenzae* type B. He suffered from recurrent bacterial infections and presented at the age of 10 a positive tuberculin skin test with negative ELISPOT assay for IFN $\gamma$  whereupon he was treated for a suspected mycobacterial infection. Despite vaccination, P4 generates no antibody-titer against

**Table 1** Immunological phenotype of P1. Analyses were directly performed after birth with patient’s cord blood and at 4 months of age. The healthy control values show the normal range in peripheral blood, as normal values for cord blood do not exist. CD, cluster of differentiation;

HSCT, hematopoietic stem cell transplantation; Ig, immunoglobulin; n.d., not detectable; OKT3, anti-CD3; PHA, phytohemagglutinin; PMA, phorbol-12-myristate-13-acetate; SAC, *Staphylococcus aureus* Cowan I

		P1	Normal range	P1	Normal range
Age		At birth (cord blood)		4 months (on day–125 before HSCT)	
Leukocytes	cells/ $\mu$ l [ $\times 10^3$ ]	23.6	8.0–15.4	–	–
Neutrophils		14.5	1.60–6.06	–	–
Eosinophils		0.33	0.12–0.66	–	–
Basophils	%	< 1	0–1	–	–
Lymphocytes	cells/ $\mu$ l [ $\times 10^3$ ]	16.2	2.07–7.53	–	–
Monocytes		4.56	0.52–1.77	–	–
Platelets	cells/ $\mu$ l [ $\times 10^5$ ]	1.71	2.18–4.19	–	–
Erythrocytes	cells/ $\mu$ l [ $\times 10^6$ ]	5.66	4.10–5.55	–	–
T cells					
CD3 <sup>+</sup>	cells/ $\mu$ l [ $\times 10^3$ ]	6.99	0.60–5.00*	11.07	2.50–5.60****
CD4 <sup>+</sup>		4.53	0.40–3.50*	7.11	1.80–4.00****
CD8 <sup>+</sup>		2.64	0.20–1.90*	3.82	0.59–1.60****
Ratio CD4/CD8		1.7	1.0–2.6*	1.86	1.70–3.90
CD3 <sup>+</sup> CD4 <sup>+</sup> CD8 <sup>–</sup> $\gamma\delta$	%	1.6	< 4	0.6	–
CD3 <sup>+</sup> CD4 <sup>+</sup> CD8 <sup>–</sup> $\alpha\beta$		0.1	–	0.5	–
CD4 <sup>+</sup> CD45RA <sup>+</sup>		98	59–100	95	77–94****
CD4 <sup>+</sup> CD45RO <sup>+</sup>		1	5–58	2.5	5–10****
CD8 <sup>+</sup> CD45RA <sup>+</sup>		97	6–100	–	–
CD8 <sup>+</sup> CD45RO <sup>+</sup>		2	0.22–100	–	–
B cells					
CD19 <sup>+</sup>	cells/ $\mu$ l [ $\times 10^3$ ]	0.18	0.04–1.10*	2.19	0.43–3.00
CD19 <sup>+</sup> CD27 <sup>+</sup>		0.04	0.009–0.14**	–	–
CD19 <sup>+</sup> CD27 <sup>+</sup> IgM <sup>+</sup> IgD <sup>+</sup>		0.03	0.001–0.04**	–	–
CD19 <sup>+</sup> CD27 <sup>+</sup> IgM <sup>–</sup> IgD <sup>–</sup>		0.001	0.005–0.07**	–	–
NK cells					
CD16 <sup>+</sup> CD56 <sup>+</sup>	cells/ $\mu$ l [ $\times 10^3$ ]	0.26	0.10–1.90*	0.37	0.10–1.30*
Immunoglobulins					
IgG	g/L	6.61	7.5–15.5	–	–
IgA	g/L	0.05	n.d.	–	–
IgM	g/L	< 0.04	0.11–0.35	–	–
IgE	IU/ml	< 0.01	0–1.5	–	–
TNF- $\alpha$ production					
LPS	pg/ml	64.60	300–2000	–	–
Lymphocyte proliferation					
w/o	cpm	3524	351***	–	–
PHA <sub>1</sub> $\mu$ g		77,498	84,417***	–	–
PHA <sub>0.1</sub> $\mu$ g		4449	16,996***	–	–
OKT3 <sub>10ng</sub>		25,031	57,729***	–	–
OKT3 <sub>1ng</sub>		8812	28,352***	–	–
SAC		68,887	26,487***	–	–
PMA <sub>10ng</sub>		193,932	58,286***	–	–
Ionomycin <sub>1</sub> $\mu$ Mol					

\*Normal range from peripheral blood [41]

\*\*Mayo Medical Laboratories, Unit Code 88800

\*\*\*Healthy day control

\*\*\*\*Normal range [42]

\*\*\*\*\*Normal range [43]

measles and presents low levels of polysaccharide-specific antibodies. P4 carries an amino acid exchange within the

LZ-domain (R319Q) and presents normal amounts of NEMO in T cells and monocytes (Fig. S2b, Table S5).

He is now 25 ½ years old, receives neither IgG-substitutions nor antibiotics and presents to our outpatient clinic in excellent health only in large intervals.

### Proliferation Assay (P1, for P2-P4 See Supplementary Data)

For analysis of T cell proliferation PBMC were stimulated with anti-CD3-coupled beads (anti-Biotin MACSiBeads, Miltenyi Biotec coupled with Biotin-anti-CD3, OKT3) at a ratio of 5:1 with and without 1 µg/ml CD28 (CD28.2, both Thermo Fisher Scientific) or with 0.5 ng/ml phorbol 12-myristate 13-acetate (PMA) and 1 µM ionomycin (Sigma Aldrich). T cell proliferation was measured by labeling PBMC with APC-H7-anti-CD3 (SK7, 1:50), APC-anti-CD4 (SK3, 1:50), PacB-anti-CD8 (RPA-T8, 1:50), and PE-anti-CD25 (M-A251, 1:25) all from BD and with 2.5 µM carboxyfluorescein succinimidyl ester (CFSE, Thermo Fisher Scientific). Data were acquired on a BD FACSCanto II flow cytometer, and data analysis was performed with FlowJo software (TreeStar). The mitogen-induced proliferation was performed as described previously [49].

### Western Blot

To determine NEMO-expression and IκBα-degradation, SV40-immortalized fibroblasts were stimulated with IL-1β (10 ng/ml) and TNF-α (20 ng/ml) for 5, 10, 15, 20, 25, and 30 min at 37 °C (for IκBα-degradation). Afterwards, cells were washed twice (PBS buffer) and centrifuged (1500 rpm, 5 min, 4 °C). Cell pellets were lysed (50 mM Tris, 150 mM NaCl, 2 mM EDTA, 0.5% Triton X, 1 × Protease inhibitor) for 20 min on ice. Lysates were collected by centrifuging (2000 rpm, 5 min, 4 °C). Protein concentration was detected with the Pierce™ BCA protein-assay-kit (Thermo Fisher Scientific). Thirty microgram protein was separated in 10% polyacrylamide-gels by standard SDS-Page. Semi-dry blotting transferred the protein on nitrocellulose membranes. The membranes were blocked (5% milk powder/TBST buffer) for 60 min at 4 °C. The first detection was performed with anti-IKKγ- (IgG-rabbit, clone EPR14660, Abcam; IgG<sub>1</sub>-mouse, clone 54, BD Biosciences; IgG-rabbit, polyclonal, Sigma-Aldrich) and anti-IκBα-polyclonal-IgG-rabbit-antibodies (C-21, Santa Cruz Biotechnology). An antibody against GAPDH (polyclonal IgG rabbit, FL-335, Santa Cruz Biotechnology) was used as intra-assay control. HRP-conjugated antibodies (goat-anti-mouse-IgG-HRP or goat-anti-rabbit-IgG-HRP, Dianova) were used for the detection of the primary antibody. The protein-antibody-complex was analyzed with ECL western blotting substrate solutions (Promega) and the ChemiDoc MP imaging system (ImageLab software 5.2.1).

## Results

### Adaptive Immunity Is Severely Impaired in P1

Immediately after birth numbers of T and B cells in cord blood of P1 were slightly elevated, yet within the normal range (Table 1). The level of γδ and αβ T cells was inconspicuous. The ratio of naïve CD45RA<sup>+</sup> to memory CD45RO<sup>+</sup> T cells (CD4<sup>+</sup>, CD8<sup>+</sup>) was markedly skewed towards naïvety. The evaluation of B cell subpopulations revealed normal amounts of total memory (CD19<sup>+</sup>CD27<sup>+</sup>) and IgM-positive memory (CD19<sup>+</sup>CD27<sup>+</sup>IgM<sup>+</sup>IgD<sup>+</sup>) cells whereas class-switched memory (CD19<sup>+</sup>CD27<sup>+</sup>IgM<sup>-</sup>IgD<sup>-</sup>) B cells were strongly reduced. IgG was slightly and IgM was markedly reduced. IgA and IgE were normal. The proliferation of CD4<sup>+</sup> and CD8<sup>+</sup> T cells upon stimulation with anti-CD3 and anti-CD3/CD28 was impaired (Fig. 3a). The lymphocyte proliferation in response to high concentrations of PHA, OKT3, SAC, and PMA/ionomycin was normal while the proliferation upon stimulation with low concentration PHA and OKT3 was reduced (Table 1). In summary, the evaluation of the adaptive immunity of P1 showed an almost complete skewing towards naïvety, impaired lymphocyte proliferation, low IgM, and reduced class-switched memory B cells.

### Impaired TNFR-, TLR-, and IL-1R-Signaling in P1

We subsequently tested the impact of the *IKBKG* mutation on the canonical NF-κB pathway by measuring the IL-6 production in patient's cord blood upon stimulation with TLR-agonists (TLR2/6-agonist PAM<sub>2</sub>CSK<sub>4</sub>, TLR4-agonist LPS) as well as IL-1β and the production of IL-10 upon activation with TNF-α. The IL-6 production upon stimulation with PAM<sub>2</sub>CSK<sub>4</sub>, LPS, and IL-1β was strongly reduced (Fig. 3b). The IL-10 production upon stimulation with TNF-α remained below the detection limit of 5 pg/ml (Fig. 3c). These results revealed strongly impaired NF-κB-dependent innate immunity.

### Splice Site Mutation IVS9 + 1G > A Leads to a Frameshift With Premature Termination Codon and Truncated NEMO Protein

We investigated the impact of the IVS9 + 1G > A mutation on the coding sequence and protein structure. The splice site mutation was not present in the data base of the exome aggregation consortium (ExAC) [50] and causes an exon 9 skipping (Fig. 4a) which induces a frameshift with premature termination codon (p. R352Sfs373X). The predicted protein is characterized by a loss of the C-terminal ZF-domain that is essential for the activation of T/B cells and NF-κB signal transduction [6, 51] (Fig. 4b). We finally analyzed the NEMO expression in patient's cord blood as well as in SV40-transformed fibroblasts. T cells as well as monocytes presented diminished

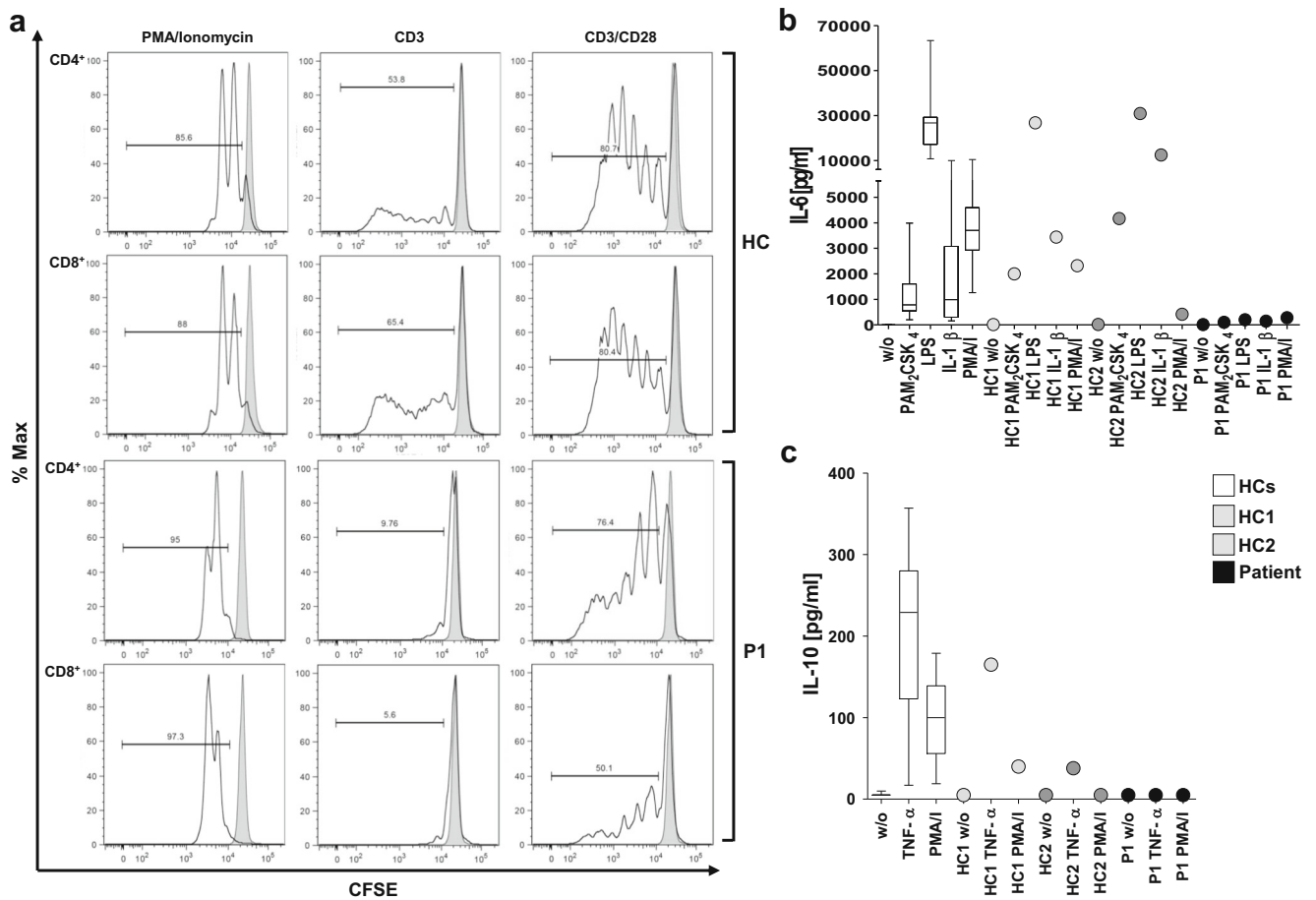


**Fig. 3** Immunological phenotype of P1. **a** T cell proliferation upon stimulation with PMA/ionomycin, CD3, and CD3/CD28 (black line). The unstimulated preparation is highlighted with a gray background. **b** IL-6 production in patient’s cord blood upon stimulation with TLR-agonists (PAM<sub>2</sub>CSK<sub>4</sub> for TLR2/TLR6, LPS for TLR4), IL-1β, and PMA/ionomycin (PMA/I) (*n* = 1). **c** IL-10 production in patient’s cord

blood upon stimulation with TNF-α and PMA/ionomycin (PMA/I) (*n* = 1). Analyses of cytokine production were performed in comparison to a healthy day (HC 1) as well as travel control (HC 2) and are depicted in comparison with all healthy controls (HCs) assessed in our laboratory (*n* = 179, whiskers 5–95 percentile)

levels of intracellular NEMO-protein in comparison with a healthy control (Fig. 4c). SV40-fibroblasts of P1 exhibited no full-length protein (48 kDa) as in a healthy control, yet a smaller NEMO-variant of approximately 41 kDa which is also present in healthy individuals but absent in the NEMO-null cell line (exon deletion, Δ 4–10) (Fig. 4d). These results suggested a strongly impaired NEMO-function.

**Splice Site Mutation IVS9 + 1G > A Impairs IκBα-Degradation and Cytokine Production in Fibroblasts**

In order to validate the impact of the mutation on the protein function, we analyzed the IL-1R- and TNFR-dependent IκBα-degradation in SV40-transformed fibroblasts. The assessment of IκBα in a cell line of a healthy subject served as a positive control whereas a NEMO null cell line functioned as a negative control. IκBα-degradation upon stimulation with IL-1β was strongly impaired and missing upon

activation with TNF-α in SV40-fibroblasts of P1 (Fig. 5a). Our results indicate that the loss of the ZF-domain strongly impairs the degradation of IκBα and the NF-κB-dependent IL-6 production upon stimulation with IL-1β and TNF-α (Fig. 5b).

**NEMO-Deficient Patients With Missense Mutations (P2-P4) Demonstrated Neither Skewing Towards Naïvety in T Cells nor Functional T Cell Impairment**

We finally assessed adaptive immunity and TNFR-, TLR-, and IL-1R-signaling in three further NEMO-deficient patients who suffered from recurrent bacterial and viral infections. P2 (D113N) and P3 (L80P) [47] presented separate amino acid exchanges within the N-terminal CC1-domain of NEMO whereas P4 demonstrated an amino acid exchange within the LZ-domain (R319Q) [48] (Fig. 6a). All patients showed neither impaired amounts of naïve T cells nor affected T cell

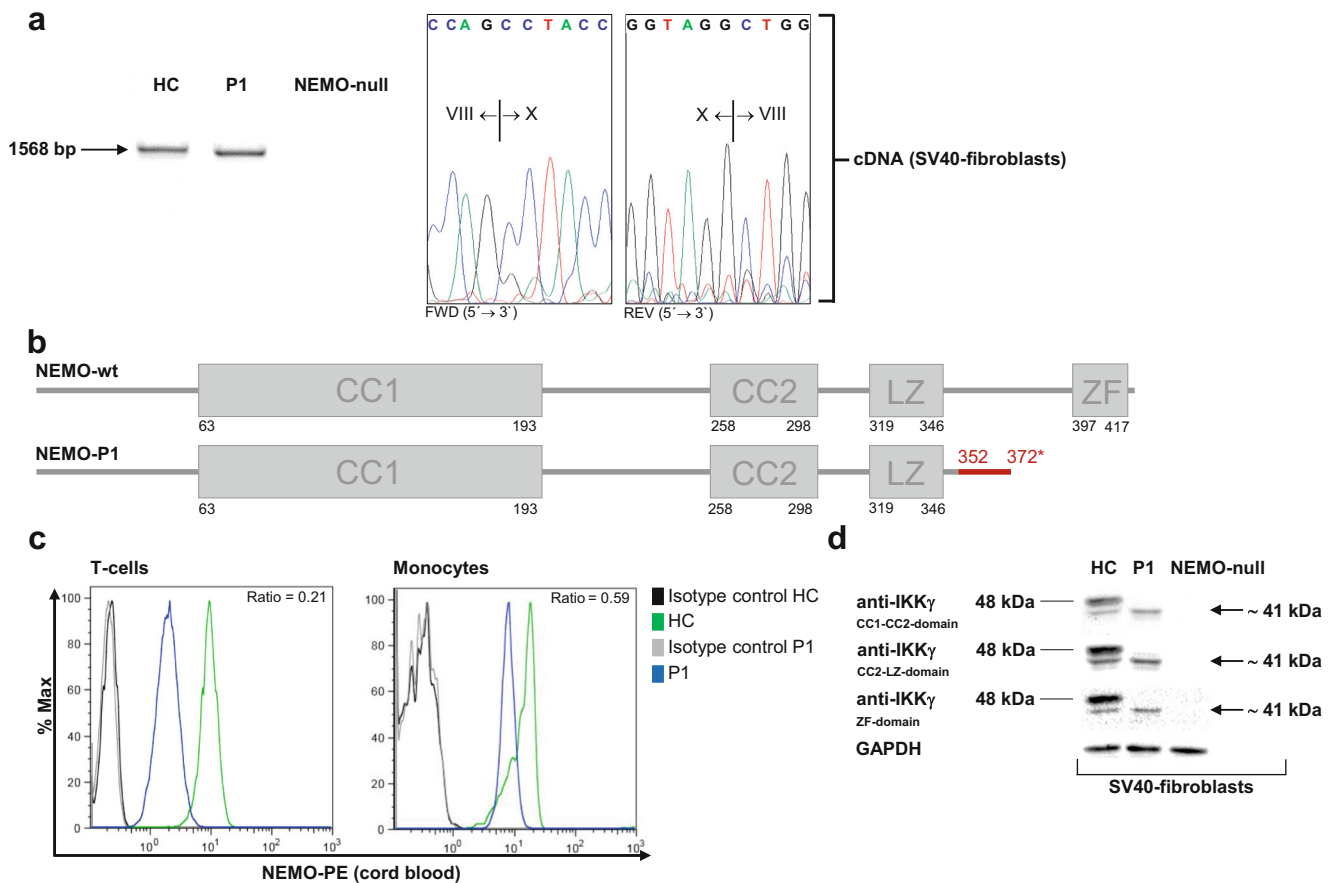


**Fig. 4** Sanger sequencing of *IKBK*G and NEMO-expression in P1. All analyses were performed in comparison with a healthy control (HC) and a NEMO-null (exon deletion,  $\Delta$  4–10) SV40-transformed fibroblast cell line. **a** Sequence analysis of the coding sequence. The coding sequence (CDS) of *IKBK*G comprises 1260 bp and was enriched by a specific RT-PCR (product size 1568 bp). The PCR product was subsequently purified and sequenced. The CDS of P1 presented a total loss of exon IX. **b** Schematic presentation of NEMO. NEMO has a length of 419 amino acids and comprises four functional domains, the coiled-coil domain CC1 and CC2, the leucine zipper (LZ), and the zinc finger (ZF) domain. The mutation of P1 leads to a frameshift with premature termination

codon at position 373 (depicted as a star) and a total loss of the C-terminal ZF-domain. wt, wild type. **c** NEMO expression in T cells and monocytes of P1 (cord blood, depicted in blue). The analysis was performed in comparison with an individual healthy control (HC, depicted in green) with an intracellular NEMO-staining and an isotype control (depicted in gray and black). The NEMO-expression was quantified by determining the ratio of the geometric means (GM, ratio = GM of P1/GM of HC). **d** NEMO expression in SV40-fibroblasts by western blot with different anti-IKK- $\gamma$ -antibodies (anti-CC1-CC2-domain, anti-CC2-LZ-domain, and anti-ZF-domain)

proliferation upon stimulation with mitogens or antigens. P2 presented reduced levels of IgG and IgG<sub>4</sub>. P3 had marginally reduced levels of IgG<sub>2</sub> but permanently reduced levels of IgM. P4 exhibited normal amounts of IgG and marginally reduced amounts of IgM (Tables S2, S4, and S5). The IL-6 production of P2 was slightly impaired upon stimulation with PAM<sub>2</sub>CSK<sub>4</sub> and IL-1 $\beta$ . P3 produced lower amounts of IL-6 upon stimulation with IL-1 $\beta$ . P4 presented no reduced IL-6 production in comparison with the control cohort and healthy day control (Fig. 6b). P2 exhibited normal amounts of IL-10 upon stimulation with TNF- $\alpha$  whereas P3 and P4 demonstrated markedly reduced levels of IL-10 (Fig. 6b). P2 and P3 are treated with regular IgG-substitution and antibiotics only if required. To date, both patients have not suffered from severe infections since the fourth and the eleventh year of age, respectively. P4 is in perfect health, off any prophylaxis.

## Discussion

NEMO deficiency was first described as causative for EDA and immunodeficiency (EDA-ID) but has soon been recognized to cause also ID without EDA, ID with mild EDA, and ID with osteopetrosis and lymphedema (EDA-ID-OL) [6–8, 36]. Correspondingly, the extent of ID in NEMO-deficient patients is highly variable and ranges from isolated susceptibility for some pathogens that decreases with age to ongoing susceptibility for life-threatening infections caused by multiple pathogens [52]. The immunological core-phenotype described in most NEMO-deficient patients (reduced levels of IgG (especially IgG<sub>2</sub>), aberrant levels of IgM and IgA, deficient polysaccharide-specific antibody responsiveness, low class-switched memory B cells, and impaired IL-10 production upon activation with TNF- $\alpha$ ) is however not predictive

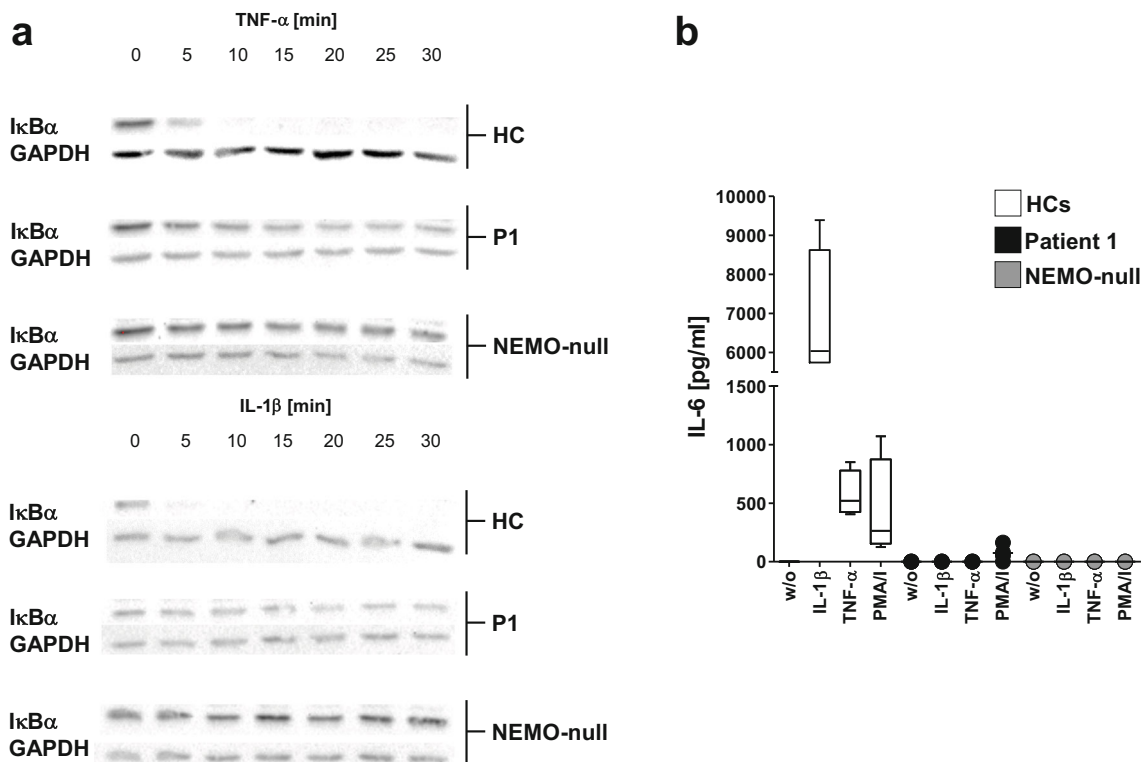


**Fig. 5** IκBα-degradation and IL-6 production of P1 upon stimulation with IL-1β and TNF-α. **a** Lysates of stimulated SV40-fibroblasts were analyzed by performing specific IRAK1, IκBα, and GAPDH western blots. Cell lines of a healthy control (HC) and a NEMO-null patient were used as intra-assay controls. **b** IL-6 production in SV40-fibroblasts upon stimulation with IL-1β, TNF-α, and PMA/Ionomycin (PMA/I) (*n* = 4).

Cell lines of healthy controls (HCs, white, whiskers 5–95 percentile) and a NEMO-null patient (gray) were used as intra-assay controls. IRAK1, IL-1 receptor-associated kinase 1; IκBα, NF-κB inhibitor α; GAPDH, glyceraldehyde-3-phosphate-dehydrogenase; IL-1β, interleukin-1β; TNF-α, tumor necrosis factor α

for the clinical course. Therefore, the definition of an immunological phenotype that predicts a severe clinical course in NEMO deficiency before chronic sequelae occur is a clinical need. The definition of a predictive immunological phenotype would help to distinguish NEMO-deficient patients for whom conservative treatment with IgG-replacement and/or anti-infective therapies is sufficient from those who should undergo HSCT as they will otherwise remain at life-long risk for severe infections.

In this report, we describe the molecular effects of a newly identified splice site mutation in the NEMO-encoding gene *IKBKG* (IVS9 + 1G > A), the resulting immunological phenotype and the clinical course in a boy whose mother has IP. The mutation leads to an exon 9 skipping with a subsequent frameshift and premature termination codon (p. R352Sfs373X) that truncates the NEMO-protein of its C-terminal ZF-domain. The loss of this domain severely impairs the production of IL-6 and IL-10 upon activation with LPS and less severely but still significantly upon activation with PAM<sub>2</sub>CSK<sub>4</sub>, IL-1β, and TNF-α in whole blood, as well as the degradation of IκBα and production of IL-6 upon activation with IL-1β and TNF-α in fibroblasts. In addition to impaired innate immunity, P1 presented features of combined immunodeficiency. P1 showed an almost complete skewing towards naïveté in

T cells, impaired lymphocyte proliferation, low IgM, and reduced class-switched memory B cells. In infancy, P1 suffered from three life-threatening infections (arthritis/sepsis caused by *Enterobacter aerogenes*, pneumonia caused by *Pneumocystis jirovecii*, and osteomyelitis caused by *Enterobacter aerogenes*).

The severe clinical course of P1 is reminiscent of two previously described NEMO-deficient patients who also presented splice site mutations within the intronic sequence of exon 9 (IVS9 – 1G > A and IVS9 + 5G > C) and truncated ZF-domains [53–55]. The first patient suffered from recurrent pneumonia and an infection caused by atypical mycobacteria. Despite immunization, he presented no detectable antibody titers against *Haemophilus influenzae* or tetanus-toxoid. IgG-substitution stabilized the clinical course for some time but “he had many difficult years thereafter and died” (personal communication J. Orange) [53, 54]. The second patient became conspicuous due to an EDA-like phenotype and a severe pneumonia already as newborn. Despite antibiotic treatment, he remained persistently bacteremic. His levels of IgM and IgG were markedly reduced as well and he expired during hospitalization [55]. The notion that NEMO-deficient patients with an impaired ZF-domain are at particularly increased risk for life-threatening infections is further supported by the

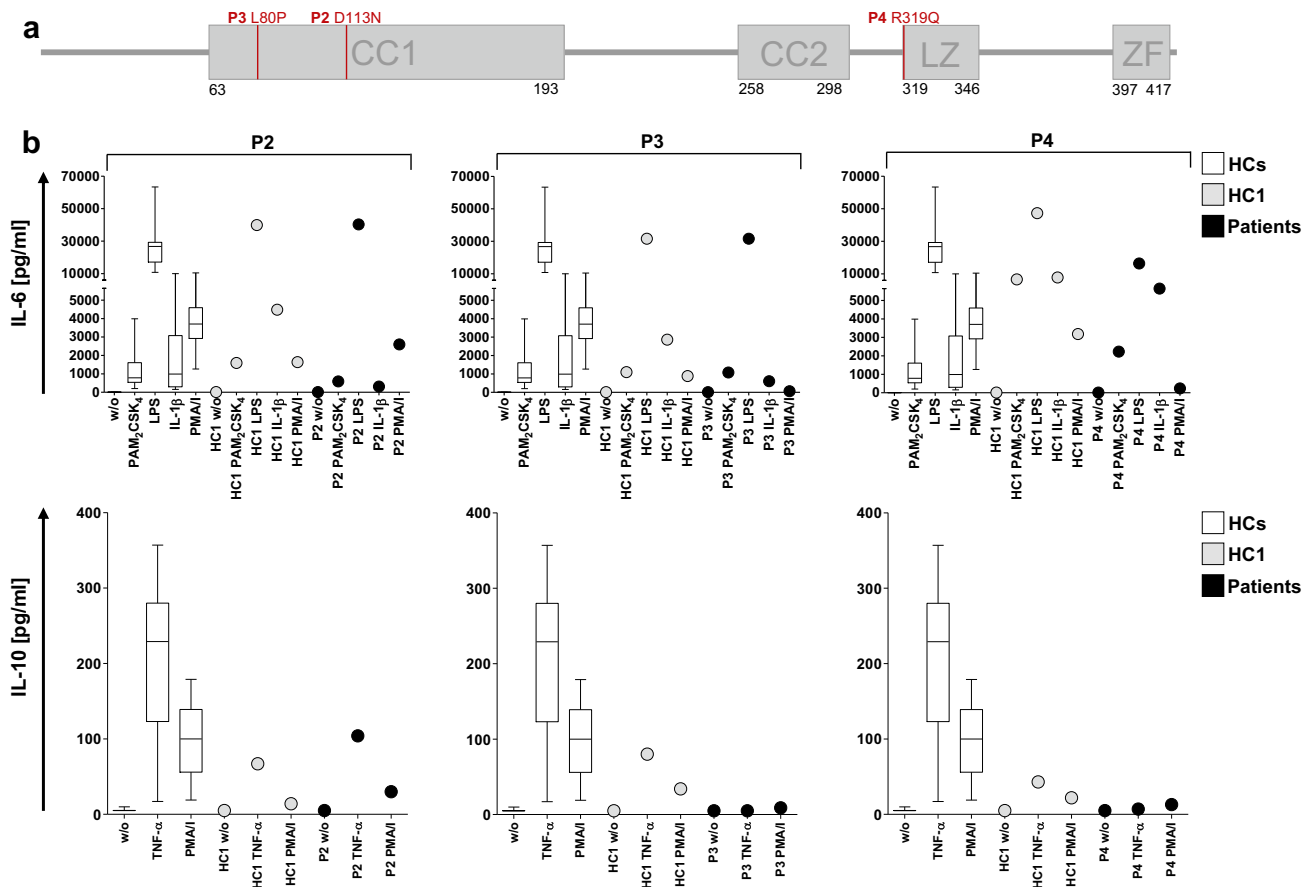


**Fig. 6** Immunological phenotype of P2–P4. **a** Schematic presentation of the missense mutations in NEMO. The mutation of P2 leads to an amino acid exchange at position 113 (p. D113N) and is located in the first coiled-coil (CC1) domain of NEMO. The mutation of P3 leads to an amino acid exchange at position 80 (p. L80P) and is also located in the CC1-domain. The mutation of P4 leads to an amino acid exchange at position 319 (p. R319Q) and is also located in the leucine zipper (LZ) domain. **b** At the top, IL-6 production in patient’s peripheral blood upon stimulation with

TLR-agonists (PAM<sub>2</sub>CSK<sub>4</sub> for TLR2/TLR6, LPS for TLR4), IL-1 $\beta$ , and PMA/ionomycin (PMA/I). At the bottom, IL-10 production in patient’s peripheral blood upon stimulation with TNF- $\alpha$  and PMA/I (P2–P4,  $n = 1$ , respectively). Analyses of cytokine production were performed in comparison to a healthy day control (HC 1) and are depicted in comparison to all healthy controls (HCs) assessed in our laboratory ( $n = 179$ , whiskers 5–95 percentile)

comparison of previously reported NEMO-deficient patients with modified or truncated ZF-domains with those whose mutations change other domains of the protein: in previously described patients impaired ZF-function seems to correlate with a complicated clinical course (Table S6) [6–8, 31, 35, 36, 56–66].

Patients with a modified protein structure concerning the CC1-, CC2-, and LZ-domain of NEMO may certainly also display severe clinical issues, however, overall present a better outcome upon antibiotic treatment and/or IgG-substitution (Table S6) [31, 32, 34, 35, 39, 44, 67, 68]. This observation is in line with the clinical presentation of P2, P3, and P4 in this report. Patient P2 suffered from recurrent bacterial and viral infections since his third month of life. His *IKBK*G mutation (c. G337A) leads to an amino acid exchange within the N-terminal CC1-domain of NEMO (D113N) that is responsible for the interaction between the  $\kappa$ B kinases IKK $\alpha$ , IKK $\beta$ , and IKK $\gamma$  (NEMO). It is debated by some whether c. G337A is

rather a polymorphism than a mutation. Although its allele frequency is rather frequent (0.009572) the resulting amino acid exchange D113N had also been previously described in females with IP [44] and in patients who displayed the immunological and clinical phenotype of NEMO deficiency [39, 45, 46]. In line with this discussion, the clinical condition of P2 improved substantially after receiving IgG-substitution and he rarely required antibiotic treatment thereafter. Even more of note, the same *IKBK*G mutation was detected in his cousin (P2C) who never developed a severe infection and is now 40 years old. P3 suffered from recurrent severe bacterial and viral infections. His mutation leads to an amino acid exchange within the CC1-domain (L80P) [47]. Similar to P2, the clinical course of P3 substantially improved upon the initiation of regular IgG-substitution. P4 carries an amino acid exchange within the LZ-domain (R319Q) that regulates the NF- $\kappa$ B signal transduction by acting as an ubiquitin binding-domain in conjunction with the domain CC2 [32, 48, 69, 70]. He

suffered from bacterial and mycobacterial infections and was temporarily treated with antibiotics but has neither been obtaining antibiotics, nor IgG-substitution since his 12th year of age, is now > 25 years old and is doing very well. In contrast to P1, P2–P4 presented with a normal ratio of CD4<sup>+</sup>CD45RA<sup>+</sup>/CD4<sup>+</sup>CD45RO<sup>+</sup> T cells and normal T cell proliferation (Tables S2, S4, and S5).

The C-terminal ZF-domain is highly conserved among species and is important for the activation of B and T cells as well as T cell proliferation [32, 71, 72]. The complete loss of this domain is associated with a reduced T cell proliferation and an impaired activation of the NF- $\kappa$ B signal transduction [6, 51]. Furthermore, NEMO-deficient patients with affected or absent ZF-domain presented stimulus-dependent impaired I $\kappa$ B $\alpha$ -degradation [32]. These observations are in line with the severely impaired NF- $\kappa$ B signaling of P1 and consistent with the immunological phenotype of I $\kappa$ B $\alpha$ -deficient patients [10]. I $\kappa$ B $\alpha$  is an inhibitor of NF- $\kappa$ B and is encoded by *NFKBIA* (*NF- $\kappa$ B inhibitor  $\alpha$* ). Activation of the trimeric IKK-complex leads to the phosphorylation and degradation of I $\kappa$ B $\alpha$  which in turn liberates NF- $\kappa$ B (Fig. 1). The first I $\kappa$ B $\alpha$ -deficient patient with an autosomal dominant variant of EDA-ID presented a hypermorphic gain-of-function mutation of *NFKBIA* causing an amino acid exchange from serine to isoleucine at position 32 (p. S32I) that prevents the phosphorylation of I $\kappa$ B $\alpha$  and causes constant retention of NF- $\kappa$ B in the cytosol [10]. By now, more than 10 patients with *NFKBIA* mutations who also presented with predominance of naïve T cells, markedly reduced memory T cells, affected TCR-mediated proliferation, and severe infections as described in NEMO-patients with truncated ZF-domain [73–77]. A similar T cell phenotype was also described in patients with homozygous mutations in *IKBKB* (IKK $\beta$ ), *CARMIL2*, *CARD11*, and *BCL10*. IKK $\beta$ - and *CARMIL2*-deficient patients suffered from severe and recurrent infections (bacterial, mycobacterial, viral and fungal) [18, 49, 78–82]. Patients with loss-of-function mutations within the *CARD11*-*BCL10*-*MALT1* (CBM)-complex caused by *CARD11*- and *BCL10* mutations suffered from severe and recurrent bacterial, mycobacterial, viral, and fungal infections [15, 16, 19, 83]. Some patients with CBM-opathies were successfully treated with HSCT [83]. To the present day, no further NEMO-deficient patient in whom naïve/memory T cells were assessed presented a skewing towards naïve CD45RA<sup>+</sup> T cells (Table S7).

In summary, our data and the review of all previously published patients suggest that NEMO-deficient patients with an affected ZF-domain suffer not only from an impaired cytokine response of innate immune cells but also from a combined immunodeficiency with impaired T and B cell function. So thorough evaluation of adaptive immunity by assessing lymphocyte subsets with a special emphasis for “skewing towards naïveté”, accompanied by assays for lymphocyte proliferation are mandatory for patients with NEMO deficiency. NEMO-

deficient patients with severely impaired T cell function are at high risk for life threatening infections and may benefit from early HSCT, whereas NEMO-deficient patients without combined immunodeficiency may rather benefit from conservative therapy. The early detailed assessment of not only the innate immunity but also of T cell function is hence mandatory as it allows to choose therapeutic options for NEMO-deficient patients stratified by the individual prognosis.

**Acknowledgements** We would like to thank all patients and their families for their trust and cooperation. We thank Christine Seib for excellent technical assistance. We thank Jean-Laurent Casanova, Anne Puel, Jacinta Bustamante, and Cheng-Lung Ku for identifying P3 and P4.

**Author Contributions** SH, UK, TM, ML, KS, FH, and HVB designed selected experiments, performed analysis, and interpreted the results. SH, UK, TM, and ML performed experiments. RK, AS, HS, AE, VW, ASch, FH, and HVB took care of the patients. NU and CM discussed data and the manuscript. SH and HVB wrote the manuscript. HVB designed the study. All authors critically revised and edited the manuscript.

**Funding Information** This work was supported by the German Federal Ministry of Education and Research (PID NET-TPA5; 01GM1111D and 01GM1517E).

## Compliance with Ethical Standards

**Conflict of Interest** The authors declare that they have no conflict of interest.

## References

- Picard C, Bobby Gaspar H, Al-Herz W, Bousfiha A, Casanova JL, Chatila T, et al. International union of immunological societies: 2017 primary immunodeficiency diseases committee report on inborn errors of immunity. *J Clin Immunol*. 2018;38(1):96–128.
- Bousfiha A, Jeddane L, Picard C, Ailal F, Bobby Gaspar H, Al-Herz W, et al. The 2017 IUIS phenotypic classification for primary immunodeficiencies. *J Clin Immunol*. 2018;38(1):129–43.
- Sen R, Baltimore D. Inducibility of kappa immunoglobulin enhancer-binding protein NF-kappa B by a posttranslational mechanism. *Cell*. 1986;47(6):921–8.
- Zhang Q, Lenardo MJ, Baltimore D. 30 years of NF-kappaB: a blossoming of relevance to human pathobiology. *Cell*. 2017;168(1–2):37–57.
- Sun SC. The non-canonical NF-kappaB pathway in immunity and inflammation. *Nat Rev Immunol*. 2017;17(9):545–58.
- Zonana J, Elder ME, Schneider LC, Orlow SJ, Moss C, Golabi M, et al. A novel X-linked disorder of immune deficiency and hypohidrotic ectodermal dysplasia is allelic to incontinentia pigmenti and due to mutations in IKK-gamma (NEMO). *Am J Hum Genet*. 2000;67(6):1555–62.
- Jain A, Ma CA, Liu S, Brown M, Cohen J, Strober W. Specific missense mutations in NEMO result in hyper-IgM syndrome with hypohidrotic ectodermal dysplasia. *Nat Immunol*. 2001;2(3):223–8.
- Doffinger R, Smahi A, Bessia C, Geissmann F, Feinberg J, Durandy A, et al. X-linked anhidrotic ectodermal dysplasia with immunodeficiency is caused by impaired NF-kappaB signaling. *Nat Genet*. 2001;27(3):277–85.

9. Picard C, Puel A, Bonnet M, Ku CL, Bustamante J, Yang K, et al. Pyogenic bacterial infections in humans with IRAK-4 deficiency. *Science*. 2003;299(5615):2076–9.
10. Courtois G, Smahi A, Reichenbach J, Doffinger R, Cancrini C, Bonnet M, et al. A hypermorphic IkappaBalpha mutation is associated with autosomal dominant anhidrotic ectodermal dysplasia and T cell immunodeficiency. *J Clin Invest*. 2003;112(7):1108–15.
11. von Bernuth H, Picard C, Jin Z, Pankla R, Xiao H, Ku CL, et al. Pyogenic bacterial infections in humans with MyD88 deficiency. *Science*. 2008;321(5889):691–6.
12. Lahtela J, Nousiainen HO, Stefanovic V, Tallila J, Viskari H, Karikoski R, et al. Mutant CHUK and severe fetal encasement malformation. *N Engl J Med*. 2010;363(17):1631–7.
13. Boisson B, Laplantine E, Prando C, Giliani S, Israelsson E, Xu Z, et al. Immunodeficiency, autoinflammation and amylopectinosis in humans with inherited HOIL-1 and LUBAC deficiency. *Nat Immunol*. 2012;13(12):1178–86.
14. Snow AL, Xiao W, Stinson JR, Lu W, Chaigne-Delalande B, Zheng L, et al. Congenital B cell lymphocytosis explained by novel germline CARD11 mutations. *J Exp Med*. 2012;209(12):2247–61.
15. Stepensky P, Keller B, Buchta M, Kienzler AK, Elpeleg O, Somech R, et al. Deficiency of caspase recruitment domain family, member 11 (CARD11), causes profound combined immunodeficiency in human subjects. *J Allergy Clin Immunol*. 2013;131(2):477–85 e1.
16. Greil J, Rausch T, Giese T, Bandapalli OR, Daniel V, Bekeredjian-Ding I, et al. Whole-exome sequencing links caspase recruitment domain 11 (CARD11) inactivation to severe combined immunodeficiency. *J Allergy Clin Immunol*. 2013;131(5):1376–83 e3.
17. Jabara HH, Ohsumi T, Chou J, Massaad MJ, Benson H, Megarbane A, et al. A homozygous mucosa-associated lymphoid tissue 1 (MALT1) mutation in a family with combined immunodeficiency. *J Allergy Clin Immunol*. 2013;132(1):151–8.
18. Pannicke U, Baumann B, Fuchs S, Henneke P, Rensing-Ehl A, Rizzi M, et al. Deficiency of innate and acquired immunity caused by an IKKB mutation. *N Engl J Med*. 2013;369(26):2504–14.
19. Torres JM, Martinez-Barricarte R, Garcia-Gomez S, Mazariegos MS, Itan Y, Boisson B, et al. Inherited BCL10 deficiency impairs hematopoietic and nonhematopoietic immunity. *J Clin Invest*. 2014;124(12):5239–48.
20. Boisson B, Laplantine E, Dobbs K, Cobat A, Tarantino N, Hazen M, et al. Human HOIP and LUBAC deficiency underlies autoinflammation, immunodeficiency, amylopectinosis, and lymphangiectasia. *J Exp Med*. 2015;212(6):939–51.
21. Zhou Q, Wang H, Schwartz DM, Stoffels M, Park YH, Zhang Y, et al. Loss-of-function mutations in TNFAIP3 leading to A20 haploinsufficiency cause an early-onset autoinflammatory disease. *Nat Genet*. 2016;48(1):67–73.
22. Zhou Q, Yu X, Demirkaya E, Deutch N, Stone D, Tsai WL, et al. Biallelic hypomorphic mutations in a linear deubiquitinase define otulipenia, an early-onset autoinflammatory disease. *Proc Natl Acad Sci U S A*. 2016;113(36):10127–32.
23. Della Mina E, Borghesi A, Zhou H, Bougarn S, Boughorbel S, Israel L, et al. Inherited human IRAK-1 deficiency selectively impairs TLR signaling in fibroblasts. *Proc Natl Acad Sci U S A*. 2017;114(4):E514–E23.
24. Israel L, Wang Y, Bulek K, Della Mina E, Zhang Z, Pedergnana V, et al. Human adaptive immunity rescues an inborn error of innate immunity. *Cell*. 2017;168(5):789–800 e10.
25. Ma CA, Stinson JR, Zhang Y, Abbott JK, Weinreich MA, Hauk PJ, et al. Germline hypomorphic CARD11 mutations in severe atopic disease. *Nat Genet*. 2017;49(8):1192–201.
26. Willmann KL, Klaver S, Dogu F, Santos-Valente E, Garncarz W, Bilic I, et al. Biallelic loss-of-function mutation in NIK causes a primary immunodeficiency with multifaceted aberrant lymphoid immunity. *Nat Commun*. 2014;5:5360.
27. Chen K, Coonrod EM, Kumanovics A, Franks ZF, Durtschi JD, Margraf RL, et al. Germline mutations in NFKB2 implicate the noncanonical NF-kappaB pathway in the pathogenesis of common variable immunodeficiency. *Am J Hum Genet*. 2013;93(5):812–24.
28. Fliegau M, Bryant VL, Frede N, Slade C, Woon ST, Lehnert K, et al. Haploinsufficiency of the NF-kappaB1 subunit p50 in common variable immunodeficiency. *Am J Hum Genet*. 2015;97(3):389–403.
29. Sharfe N, Merico D, Karanxha A, Macdonald C, Dadi H, Ngan B, et al. The effects of RelB deficiency on lymphocyte development and function. *J Autoimmun*. 2015;65:90–100.
30. Badran YR, Dedeoglu F, Leyva Castillo JM, Bainter W, Ohsumi TK, Bousvaros A, et al. Human RELA haploinsufficiency results in autosomal-dominant chronic mucocutaneous ulceration. *J Exp Med*. 2017;214(7):1937–47.
31. Hanson EP, Monaco-Shawver L, Solt LA, Madge LA, Banerjee PP, May MJ, et al. Hypomorphic nuclear factor-kappaB essential modulator mutation database and reconstitution system identifies phenotypic and immunologic diversity. *J Allergy Clin Immunol*. 2008;122(6):1169–77 e16.
32. Shifera AS. The zinc finger domain of IKKgamma (NEMO) protein in health and disease. *J Cell Mol Med*. 2010;14(10):2404–14.
33. Kawai T, Nishikomori R, Izawa K, Murata Y, Tanaka N, Sakai H, et al. Frequent somatic mosaicism of NEMO in T cells of patients with X-linked anhidrotic ectodermal dysplasia with immunodeficiency. *Blood*. 2012;119(23):5458–66.
34. Fusco F, Pescatore A, Conte MI, Mirabelli P, Paciolla M, Esposito E, et al. EDA-ID and IP, two faces of the same coin: how the same IKBKKG/NEMO mutation affecting the NF-kappaB pathway can cause immunodeficiency and/or inflammation. *Int Rev Immunol*. 2015;34(6):445–59.
35. Fusco F, Pescatore A, Bal E, Ghoul A, Paciolla M, Lioi MB, et al. Alterations of the IKBKKG locus and diseases: an update and a report of 13 novel mutations. *Hum Mutat*. 2008;29(5):595–604.
36. Smahi A, Courtois G, Vabres P, Yamaoka S, Heuert S, Munnich A, et al. Genomic rearrangement in NEMO impairs NF-kappaB activation and is a cause of incontinentia pigmenti. The International Incontinentia Pigmenti (IP) Consortium. *Nature*. 2000;405(6785):466–72.
37. Makris C, Godfrey VL, Krahn-Sentleben G, Takahashi T, Roberts JL, Schwarz T, et al. Female mice heterozygous for IKK gamma/NEMO deficiencies develop a dermatopathy similar to the human X-linked disorder incontinentia pigmenti. *Mol Cell*. 2000;5(6):969–79.
38. Courtois G, Israel A. NF-kappa B defects in humans: the NEMO/incontinentia pigmenti connection. *Sci STKE* 2000;2000(58):pe1.
39. Miot C, Imai K, Imai C, Mancini AJ, Kucuk ZY, Kawai T, et al. Hematopoietic stem cell transplantation in 29 patients hemizygous for hypomorphic IKBKKG/NEMO mutations. *Blood*. 2017;130(12):1456–67.
40. Klemann C, Pannicke U, Morris-Rosendahl DJ, Vlantis K, Rizzi M, Uhlig H, et al. Transplantation from a symptomatic carrier sister restores host defenses but does not prevent colitis in NEMO deficiency. *Clin Immunol*. 2016;164:52–6.
41. Comans-Bitter WM, de Groot R, van den Beemd R, Neijens HJ, Hop WC, Groeneveld K, et al. Immunophenotyping of blood lymphocytes in childhood. Reference values for lymphocyte subpopulations. *J Pediatr*. 1997;130(3):388–93.
42. Shearer WT, Rosenblatt HM, Gelman RS, Oyomopito R, Plaeger S, Stiehm ER, et al. Lymphocyte subsets in healthy children from birth through 18 years of age: the pediatric AIDS Clinical Trials Group P1009 study. *J Allergy Clin Immunol*. 2003;112(5):973–80.
43. van Gent R, van Tilburg CM, Nibbelke EE, Otto SA, Gaiser JF, Janssens-Korpela PL, et al. Refined characterization and reference values of the pediatric T- and B-cell compartments. *Clin Immunol*. 2009;133(1):95–107.

44. Fusco F, Bardaro T, Fimiani G, Mercadante V, Miano MG, Falco G, et al. Molecular analysis of the genetic defect in a large cohort of IP patients and identification of novel NEMO mutations interfering with NF-kappaB activation. *Hum Mol Genet.* 2004;13(16):1763–73.
45. Salt BH, Niemela JE, Pandey R, Hanson EP, Deering RP, Quinones R, et al. IKBKG (nuclear factor-kappa B essential modulator) mutation can be associated with opportunistic infection without impairing toll-like receptor function. *J Allergy Clin Immunol.* 2008;121(4):976–82.
46. Abbott JK, Quinones RR, de la Morena MT, Gelfand EW. Successful hematopoietic cell transplantation in patients with unique NF-kappaB essential modulator (NEMO) mutations. *Bone Marrow Transplant.* 2014;49(11):1446–7.
47. Ku CL, Dupuis-Girod S, Dittrich AM, Bustamante J, Santos OF, Schulze I, et al. NEMO mutations in 2 unrelated boys with severe infections and conical teeth. *Pediatrics.* 2005;115(5):e615–9.
48. Filipe-Santos O, Bustamante J, Haverkamp MH, Vinolo E, Ku CL, Puel A, et al. X-linked susceptibility to mycobacteria is caused by mutations in NEMO impairing CD40-dependent IL-12 production. *J Exp Med.* 2006;203(7):1745–59.
49. Schober T, Magg T, Laschinger M, Rohlf M, Linhares ND, Puchalka J, et al. A human immunodeficiency syndrome caused by mutations in CARMIL2. *Nat Commun.* 2017;8:14209.
50. Lek M, Karczewski KJ, Minikel EV, Samocha KE, Banks E, Fennell T, et al. Analysis of protein-coding genetic variation in 60,706 humans. *Nature.* 2016;536(7616):285–91.
51. Pachlopnik Schmid JM, Junge SA, Hossle JP, Schneider EM, Roosnek E, Seger RA, et al. Transient hemophagocytosis with deficient cellular cytotoxicity, monoclonal immunoglobulin M gammopathy, increased T-cell numbers, and hypomorphic NEMO mutation. *Pediatrics.* 2006;117(5):e1049–56.
52. Picard C, Casanova JL, Puel A. Infectious diseases in patients with IRAK-4, MyD88, NEMO, or IkappaBalpha deficiency. *Clin Microbiol Rev.* 2011;24(3):490–7.
53. Orange JS, Jain A, Ballas ZK, Schneider LC, Geha RS, Bonilla FA. The presentation and natural history of immunodeficiency caused by nuclear factor kappaB essential modulator mutation. *J Allergy Clin Immunol.* 2004;113(4):725–33.
54. Orange JS, Levy O, Brodeur SR, Krzewski K, Roy RM, Niemela JE, et al. Human nuclear factor kappa B essential modulator mutation can result in immunodeficiency without ectodermal dysplasia. *J Allergy Clin Immunol.* 2004;114(3):650–6.
55. Johnston AM, Niemela J, Rosenzweig SD, Fried AJ, Delmonte OM, Fleisher TA, et al. A novel mutation in IKBKG/NEMO leads to ectodermal dysplasia with severe immunodeficiency (EDA-ID). *J Clin Immunol.* 2016;36(6):541–3.
56. Aradhya S, Courtois G, Rajkovic A, Lewis RA, Levy M, Israel A, et al. Atypical forms of incontinentia pigmenti in male individuals result from mutations of a cytosine tract in exon 10 of NEMO (IKK-gamma). *Am J Hum Genet.* 2001;68(3):765–71.
57. Dupuis-Girod S, Corradini N, Hadj-Rabia S, Fournet JC, Faivre L, Le Deist F, et al. Osteopetrosis, lymphedema, anhidrotic ectodermal dysplasia, and immunodeficiency in a boy and incontinentia pigmenti in his mother. *Pediatrics.* 2002;109(6):e97.
58. Orange JS, Brodeur SR, Jain A, Bonilla FA, Schneider LC, Kretschmer R, et al. Deficient natural killer cell cytotoxicity in patients with IKK-gamma/NEMO mutations. *J Clin Invest.* 2002;109(11):1501–9.
59. Nishikomori R, Akutagawa H, Maruyama K, Nakata-Hizume M, Ohmori K, Mizuno K, et al. X-linked ectodermal dysplasia and immunodeficiency caused by reversion mosaicism of NEMO reveals a critical role for NEMO in human T-cell development and/or survival. *Blood.* 2004;103(12):4565–72.
60. Martinez-Pomar N, Munoz-Saa I, Heine-Suner D, Martin A, Smahi A, Matamoros N. A new mutation in exon 7 of NEMO gene: late skewed X-chromosome inactivation in an incontinentia pigmenti female patient with immunodeficiency. *Hum Genet.* 2005;118(3–4):458–65.
61. Cheng LE, Kanwar B, Tcheurekdjian H, Grenert JP, Muskat M, Heyman MB, et al. Persistent systemic inflammation and atypical enterocolitis in patients with NEMO syndrome. *Clin Immunol.* 2009;132(1):124–31.
62. Haverkamp MH, Marciano BE, Frucht DM, Jain A, van de Vosse E, Holland SM. Correlating interleukin-12 stimulated interferon-gamma production and the absence of ectodermal dysplasia and anhidrosis (EDA) in patients with mutations in NF-kappaB essential modulator (NEMO). *J Clin Immunol.* 2014;34(4):436–43.
63. Ramirez-Alejo N, Alcantara-Montiel JC, Yamazaki-Nakashimada M, Duran-McKinster C, Valenzuela-Leon P, Rivas-Larrauri F, et al. Novel hypomorphic mutation in IKBKG impairs NEMO-ubiquitylation causing ectodermal dysplasia, immunodeficiency, incontinentia pigmenti, and immune thrombocytopenic purpura. *Clin Immunol.* 2015;160(2):163–71.
64. Wu S, Orange JS, Chiou EH, Nicholas SK, Seeborg F, Gwalani LA, et al. Use of enteral immunoglobulin in NEMO syndrome for eradication of persistent symptomatic norovirus enteritis. *J Allergy Clin Immunol Pract.* 2016;4(3):539–41 e1.
65. Jorgensen SE, Bottger P, Kofod-Olsen E, Holm M, Mork N, Orntoft TF, et al. Ectodermal dysplasia with immunodeficiency caused by a branch-point mutation in IKBKG/NEMO. *J Allergy Clin Immunol.* 2016;138(6):1706–9 e4.
66. Yu JC, Khodadadi H, Malik A, Davidson B, Salles E, Bhatia J, et al. Innate Immunity of Neonates and Infants. *Front Immunol.* 2018;9:1759.
67. Orange JS, Levy O, Geha RS. Human disease resulting from gene mutations that interfere with appropriate nuclear factor-kappaB activation. *Immunol Rev.* 2005;203:21–37.
68. Courtois G, Gilmore TD. Mutations in the NF-kappaB signaling pathway: implications for human disease. *Oncogene.* 2006;25(51):6831–43.
69. Ivins FJ, Montgomery MG, Smith SJ, Morris-Davies AC, Taylor IA, Rittinger K. NEMO oligomerization and its ubiquitin-binding properties. *Biochem J.* 2009;421(2):243–51.
70. Clark K, Nanda S, Cohen P. Molecular control of the NEMO family of ubiquitin-binding proteins. *Nat Rev Mol Cell Biol.* 2013;14(10):673–85.
71. Tang ED, Wang CY, Xiong Y, Guan KL. A role for NF-kappaB essential modifier/IkappaB kinase-gamma (NEMO/IKKgamma) ubiquitination in the activation of the IkappaB kinase complex by tumor necrosis factor-alpha. *J Biol Chem.* 2003;278(39):37297–305.
72. Cordier F, Grubisha O, Traincard F, Veron M, Delepierre M, Agou F. The zinc finger of NEMO is a functional ubiquitin-binding domain. *J Biol Chem.* 2009;284(5):2902–7.
73. Schimke LF, Rieber N, Rylaarsdam S, Cabral-Marques O, Hubbard N, Puel A, et al. A novel gain-of-function IKBA mutation underlies ectodermal dysplasia with immunodeficiency and polyendocrinopathy. *J Clin Immunol.* 2013;33(6):1088–99.
74. Yoshioka T, Nishikomori R, Hara J, Okada K, Hashii Y, Okafuji I, et al. Autosomal dominant anhidrotic ectodermal dysplasia with immunodeficiency caused by a novel NFKBIA mutation, p.Ser36Tyr, presents with mild ectodermal dysplasia and non-infectious systemic inflammation. *J Clin Immunol.* 2013;33(7):1165–74.
75. Boisson B, Puel A, Picard C, Casanova JL. Human IkappaBalpha gain of function: a severe and syndromic immunodeficiency. *J Clin Immunol.* 2017;37(5):397–412.
76. Staples E, Morillo-Gutierrez B, Davies J, Petersheim D, Massaad M, Slatter M, et al. Disseminated Mycobacterium mageritense and Salmonella infections associated with a novel variant in NFKBIA. *J Clin Immunol.* 2017;37(5):415–8.

77. Moriya K, Sasahara Y, Ohnishi H, Kawai T, Kanegane H. IKBA S32 mutations underlie ectodermal dysplasia with immunodeficiency and severe noninfectious systemic inflammation. *J Clin Immunol*. 2018;38(5):543–5.
78. Nielsen C, Jakobsen MA, Larsen MJ, Muller AC, Hansen S, Lillevang ST, et al. Immunodeficiency associated with a nonsense mutation of IKBKB. *J Clin Immunol*. 2014;34(8):916–21.
79. Sorte HS, Osnes LT, Fevang B, Aukrust P, Erichsen HC, Backe PH, et al. A potential founder variant in CARMIL2/RLTPR in three Norwegian families with warts, molluscum contagiosum, and T-cell dysfunction. *Mol Genet Genomic Med*. 2016;4(6):604–16.
80. Alazami AM, Al-Helale M, Alhissi S, Al-Saud B, Alajlan H, Monies D, et al. Novel CARMIL2 mutations in patients with variable clinical dermatitis, infections, and combined immunodeficiency. *Front Immunol*. 2018;9:203.
81. Cardinez C, Miraghazadeh B, Tanita K, da Silva E, Hoshino A, Okada S, et al. Gain-of-function IKBKB mutation causes human combined immune deficiency. *J Exp Med*. 2018;215(11):2715–24.
82. Cuvelier GDE, Rubin TS, Junker A, Sinha R, Rosenberg AM, Wall DA, et al. Clinical presentation, immunologic features, and hematopoietic stem cell transplant outcomes for IKBKB immune deficiency. *Clin Immunol*. 2018.
83. Lu HY, Bauman BM, Arjunaraja S, Dotjbal B, Milner JD, Snow AL, et al. The CBM-opathies—a rapidly expanding Spectrum of human inborn errors of immunity caused by mutations in the CARD11-BCL10-MALT1 complex. *Front Immunol*. 2018;9:2078.

**Publisher's Note** Springer Nature remains neutral with regard to jurisdictional claims in published maps and institutional affiliations.